Molecular Crystals and Liquid Crystals
Publication details, including instructions for authors and subscription information:
http://www.tandfonline.com/loi/gmcl16

D.C. Photoconductivity of Para-Terphenyl

J. Gonzalez-basurto [a] , A. Diaz-gongora [a] , Z. Burshtein [b] & D. F. Williams [c]

[a] Escuela de Fisica, I.P.N., Mexico City, Mexico

[b] Racah Institute of Physics, The Hebrew University, Jerusalem, 91000, Israel

[c] Division of Chemistry, National Research Council of Canada, Ottawa, Canada, K1A OR6

Version of record first published: 28 Mar 2007.

To cite this article: J. Gonzalez-basurto , A. Diaz-gongora , Z. Burshtein & D. F. Williams (1979): D.C. Photoconductivity of Para-Terphenyl, Molecular Crystals and Liquid Crystals, 51:3-4, 303-316

To link to this article: http://dx.doi.org/10.1080/00268947908084716

Mol. Cryst. Liq. Cryst., 1979, Vol. 51, pp. 303–316

Printed in Holland

D.C. Photoconductivity of Para-Terphenyl

J. GONZALEZ-BASURTO and A. DIAZ-GONGORA

Escuela de Fisica, I.P.N. Mexico City, Mexico

and

Z. BURSHTEIN

Racah Institute of Physics, The Hebrew University, Jerusalem 91000, Israel

and

D. F. WILLIAMS

Division of Chemistry, National Research Council of Canada, Ottawa, Canada K1A 0R6

(*Received November 2, 1978*)

D.C. photoconductivity characteristics of *p*-terphenyl single crystals have been measured in the near U.V. Holes and electrons are found to be produced at approximately equal rates which are proportional to the 3/2 power of the ight intensity. The spectra show a fast exponential rise of the photocurrents (40–50 times) in the photon energy range 3.5–3.73 eV and then a plateau up to 4.25 eV. **b** polarized light is 6–9 times more efficient in carrier generation compared to the **a** polarized light. The high field voltage and temperature effects on carrier generation are found to be in agreement with the basic predictions of Onsager's theory.

I INTRODUCTION

The interest in organics as materials for photoconductive or photovoltaic devices has resulted in numerous studies of electronic properties of these materials. The studies have involved two basic problems, carrier generation and carrier mobility. In organic materials the understanding of carrier generation is complicated when compared to the simple inorganic semiconductors. Direct band-to-band optical transitions often take place only at high photon energies, and hence they are masked by lower energy excitonic transitions. The latter may eventually result in free carrier production

through secondary processes e.g., exciton interaction with bulk traps,[1] surface states[2] or through multi-excitonic interactions.[3] In some studies, the close relation between photo-currents and excitonic optical transitions served to obtain the excitonic absorption structure. This method is limited to cases where carrier production is a result of the exciton interaction with traps or surface states. For other carrier production processes there is no simple or general relation between the photocurrent spectrum and the excitonic transition structure.

Some recent progress in the understanding of carrier generation in organic crystals[4] has been through the application of Onsager's theory[5] to describe the electric field and temperature effects on the electron-hole dissociation probability. So far the theory has been found satisfactory in describing carrier generation for pulsed photoconductivity of anthracene[4] and *p*-terphenyl.[6] Our present paper on d.c. photoconductivity of *p*-terphenyl is in some respects complementary to the previous work concerning pulsed photoconductivity of the same material.[6]

II EXPERIMENTAL

Para-terphenyl single crystals were grown from the melt by the Bridgman method. The starting material was commercial *p*-terphenyl initially purified by chromatography through an alumina column, and then by zone refining for about 30 zone passes. Samples of typical dimensions $5 \times 5 \times 2$ mm^3 were cut from the ingot parallel to the (a, b) plane by a wire saw, and polished on a fine cloth soaked with a mixture of water and alumina powder to form a thin ($\sim$0.2 mm) platelet. Crystallographic orientation of the samples was obtained by standard X-ray techniques. The platelets were mounted between a transparent conducting quartz plate (SnO_2 coated), which served as the front electrode through which the crystal was illuminated, and mercury which served as the back electrode. The crystal holder was mounted in a cryogenic system, where the temperature could be varied between 150°K and 300°K, and kept under vacuum of 10^{-5} torr. A copper-constantan thermocouple attached to the crystal holder monitored the temperature.

The optical system consisted of a 1000W Oriel Xe arc lamp followed by a Hilger & Watts Monospex 600 monochromator. To obtain polarized light we used a B. Halle U.V. polarizer mounted between the monochromator exit slit and the cryostat window. The light intensity was calibrated against an Eppley calibrated thermopile. The high voltage across the crystal was provided by a 240 A Kiethley High-Voltage power supply. The photocurrents were measured by a Kiethley model 610B electrometer and recorded by a Hewlett–Packard 7132 recorder.

III RESULTS AND DISCUSSION

Like the other aromatic hydrocarbons, *p*-terphenyl is insulating in the dark.[7] Photocurrents appear with illumination of wavelengths $\lambda \lesssim 3600$ Å. The wavelength threshold for the appearance of these photocurrents corresponds to the onset of the strong crystal absorption. Singlet absorption is known to start at wavelengths $\lambda \lesssim 3600$ Å from comparison of the fluorescence spectra viewed from the front or from the back of the illuminated surface,[8] but the detailed spectrum has not been measured yet. Typical singlet-singlet absorption coefficients in organic crystals[7] are of the order of 10^5 cm^{-1}, thus in this wavelength region the light is fully absorbed in a region about 0.1 thick at the illiminated surface. This region then acts as a source of free carriers. With the illuminated surface positive or negative, free holes or electrons, respectively, are swept into the crystal bulk. In Figs. 1 and 2 we show the hole and electron photocurrent spectra, respectively,

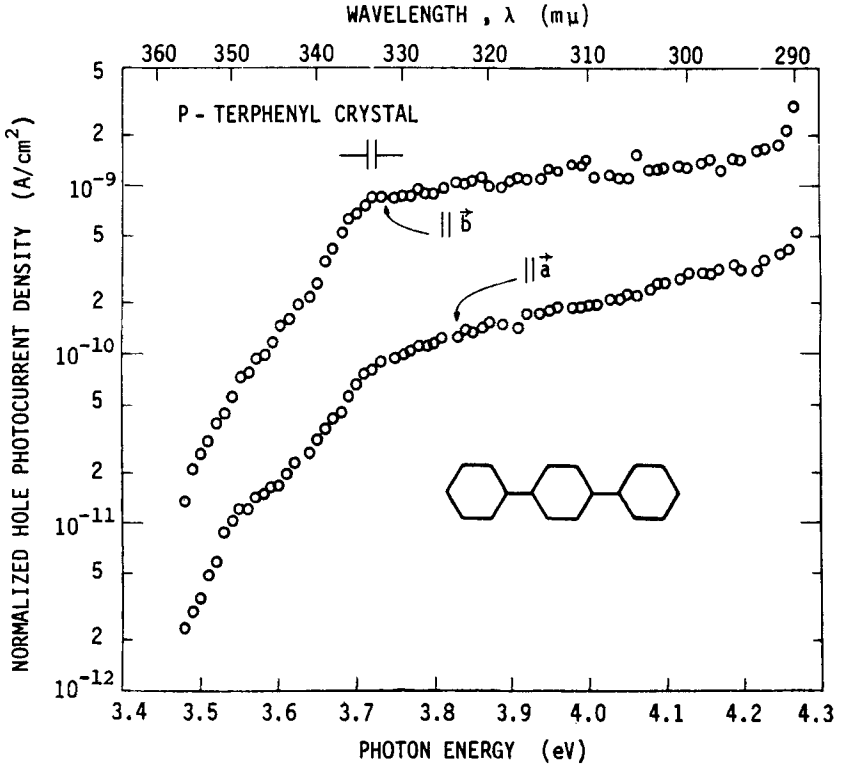

FIGURE 1 Semi-log plot of hole photocurrent vs. photon energy normalized to a photon flux $F = 3.6 \times 10^{13}$ photons cm^{-2} sec^{-1}. Voltage of 300 V applied across 0.15 mm thick sample normal to (*a*, *b*) plane at room temperature. Insert shows the molecular structure of *p*-terphenyl.

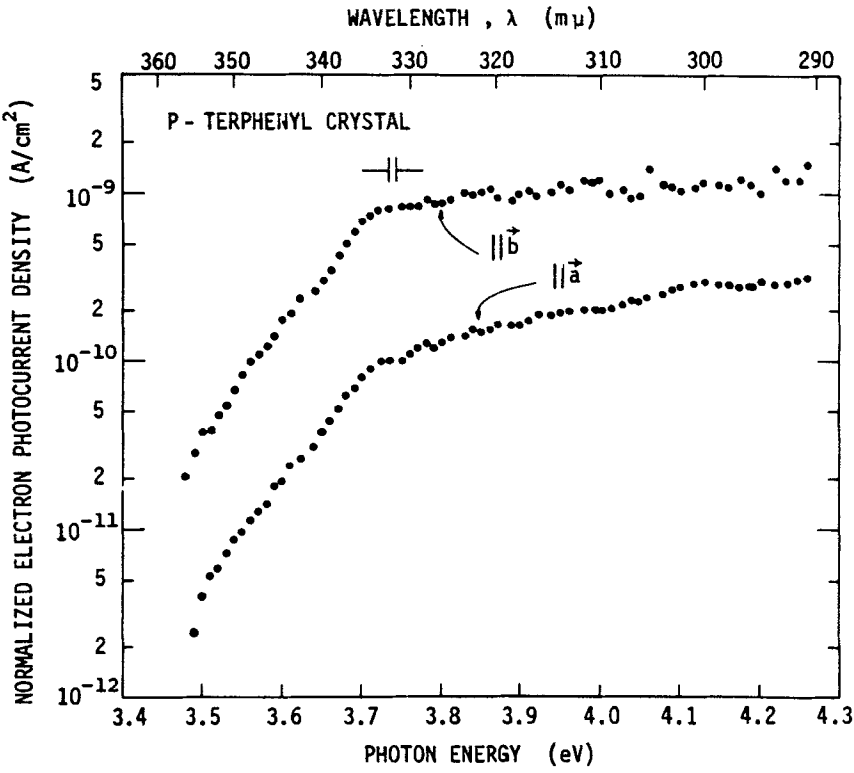

FIGURE 2 Semi-log plot of electron photocurrent vs. photon energy. Conditions same as for Figure 1.

each for light polarized either along the **a** or **b** crystallographic directions,[9,10] with the electric field applied normal to the (*a*, *b*) plane. As will be shown later, the applied field was sufficient for both types of photogenerated charge carriers to almost completely overcome bulk trapping as well as surface recombination. The photocurrents must then reflect the generation rates of the corresponding carriers. In fact, some slow carrier trapping occurs during illumination; the photocurrents decay within 20–30 sec after the onset of illumination to about 80% of their initial value (then they remain approximately constant). This decay is due to electric polarization of the crystal opposing the external voltage, and effect which is always associated with excess carrier trapping. The crystal polarization could be removed by illuminating the crystal while the electrodes were short-circuited. The data shown in Figures 1 and 2, as well as in all the other figures, correspond to the initial photocurrent signals as measured during 2–3 sec immediately

after the onset of illumination. The crystals were depolarized between each successive measurements.

It is seen in Figures 1 and 2 that holes and electrons are produced at approximately equal rates throughout the entire spectral range, and that **b** polarized light is 6–9 times more efficient in carrier generation compared to **a** polarized light. The spectral shapes, however, for both light polarizations are essentially the same, and no energy splitting can be detected in the present resolution. The photocurrents rise more or less exponentially 40–50 times in the photon energy range 3.5–3.73 eV (the photocurrent tail) and this fast rise is followed by a plateau, where the photocurrents rise by less than a factor of 2 up to the highest photon energy measured (4.26 eV). These spectra are consistent with an early measurement of photoconductivity of *p*-terphenyl utilizing surface-type cells.[11] Though the appearance of photocurrents for $\lambda \lesssim 3600$ Å coincides with the singlet 0–0 optical transition,[12] it is not clear whether the rest of the photocurrent spectra reflect, to any extent, the singlet-singlet optical transitions. The singlet fluorescence emission spectrum of the crystal[12] shows distinct, well resolved peaks, reflecting a molecular vibrational mode of 0.16 eV. A structure corresponding to the same vibrational mode is expected to show up in the singlet excitation spectrum. No such structure is apparent in the photocurrent spectra. It should be noted that singlet excitons produced in this energy region do not have sufficient energy to dissociate and produce free carriers, hence a secondary process must be involved. In anthracene, as well as in several other molecular crystals, the crystal singlet absorption is reflected in the photocurrent spectra, for the singlet excitons produced dissociate through surface states.[7] Dissociation in the bulk could be very complex involving multi-excitonic processes,[3] which would be seen by a high power dependence of the photocurrent on the light intensity.

In Figure 3 we present measurements of the light intensity dependence of the photocurrents. The hole and electron photocurrent densities are plotted vs light intensity on a log-log scale. The photon energies given are 3.62 eV, in the tail region of the photocurrents, and 3.73 eV, at about the beginning of the plateau (Figures 1 and 2). Here, as well as for other wavelengths throughout the entire spectral range (3.5–4.3 eV) the slopes are always 1.5, namely, the photocurrents are proportional to the 1.5 power of the light intensity. The normalization of the photocurrent spectra of Figures 1 and 2 was carried out accordingly. It is obvious then that the generation of a pair of free carriers involves more than one photon or one exciton.

In a previous work[6] pulsed conductivity of *p*-terphenyl crystals was measured utilizing short light pulses ($\sim 10^{-8}$ sec) from a nitrogen laser ($\lambda = 3371$ Å). The initial photocurrent varied as the square of the light

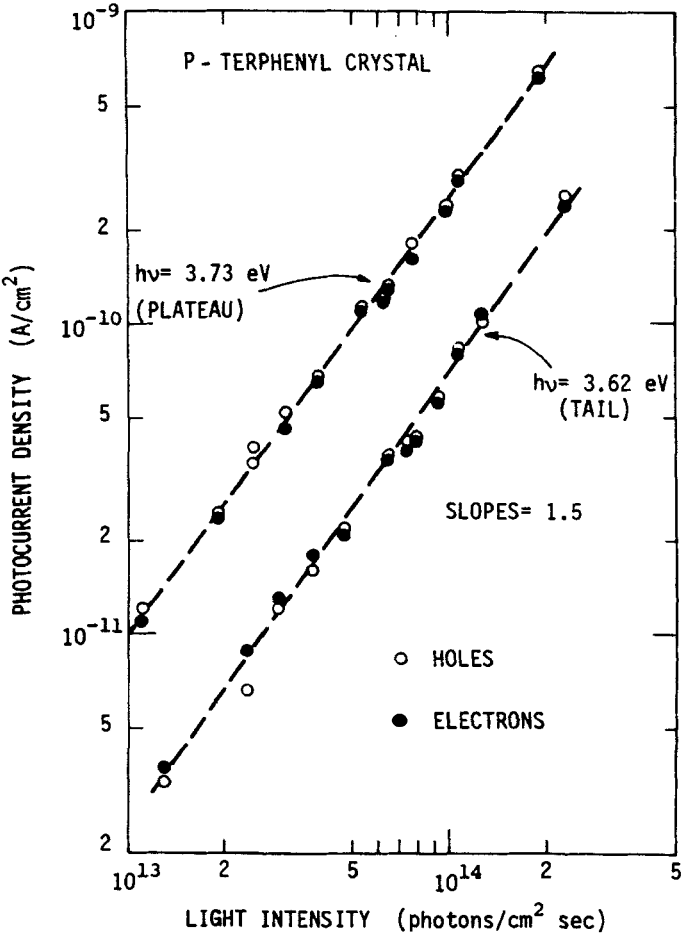

FIGURE 3 Log-log plots of hole and electron photocurrents (open and full circles, respectively) vs. unpolarized light intensity, for two different photon energies. Voltage of 300 V applied across 0.15 mm thick sample normal to (*a*, *b*) plane at room temperature.

intensity, and at room temperature it was expressed as $J(t=0) \approx 10^{-30} qF^2 \tau t_t^{-1}$ (A/cm^2), where q is the electronic charge, F is the photon flux density (in units of photons/cm^2 sec), τ is the duration of the light pulse and t_t is the transit-time of the photo-generated carriers across the sample. For continuous illumination the maximum photocurrent density of the same photogeneration process would be given by setting $\tau t_t^{-1} \approx 1$. The photocurrent density for light intensities of the order used in the present work ($\sim 10^{14}$ photons/cm^2 sec, see Figure 3) would be only of the order of 10^{-21} A/cm^2 (!). This is more than ten orders of magnitude smaller than the

actual photocurrent densities we measured with continuous illumination. It is obvious then that a different charge-carrier generation mechanism is dominant for continuous illumination. The similarity between the hole and electron production rates suggests an intrinsic process, though this need not necessarily be the case. In anthracence, for example, the major photogeneration process for strongly absorbed light involves the interaction of photo-generated singlet excitons with surface traps, which results in different rates for free hole and free electron production[7] unless the surfaces are very specially prepared.

The present results suggest two possible processes yielding the observed light intensity dependence. (i) free carrier generation via bimolecular interaction of photogenerated singlet excitons with triplet excitons, where triplet excitons are produced by intersystem crossing,[13] from the singlet manifold, (ii) photoionization of the triplet excitons produced. Neglecting diffusion of singlet, as well as triplet excitons, the rate equation governing the concentration of triplet excitons T can be approximated as[14]

$$dT/dt = f\alpha_S F - \beta_T T - \gamma_T T^2, \tag{1}$$

where α_S is the singlet-singlet absorption coefficient, f is the fraction of photogenerated singlet excitons that undergo intersystem crossing to the triplet manifold, β_T is the triplet monomolecular decay rate constant and γ_T is the triplet bimolecular decay rate constant.[14] To the best of our knowledge, the values of the above parameters have not been measured for *p*-terphenyl, therefore, we assume their order of magnitude to be similar to those of anthracene,[14] a good assumption considering the strong resemblance in molecular structure. fluorescence efficiency and singlet transition energy levels. Thus we have $\alpha_S \sim 10^5\ \text{cm}^{-1}$, $f \sim 10^{-2}$, $\beta_T \sim 10^2\ \text{sec}^{-1}$ and $\gamma_T \sim 10^{-11}\ \text{cm}^3\ \text{sec}^{-1}$. At low light intensities the triplet population is controlled by the triplet monomolecular decay rate, while for high light intensities hence high triplet densities bimolecular decay becomes dominant. With these values given above for light intensities larger than the order of 10^{12} photons/cm^2 sec, triplet bimolecular decay dominates and such is the experimental condition studied here. Steady-state conditions are established several milliseconds after the onset of the illumination, and the corresponding triplet excitons concentration T_{ss} is then expressed by

$$T_{ss} \simeq (f\alpha_S/\gamma_T)^{1/2} F^{1/2}. \tag{2}$$

The singlet exciton concentration under the present illumination conditions is governed by the singlet monomolecular decay rate $\beta_s(\beta_s^{-1} = 5.5 \times 10^{-9}$ sec)[12] the rate equation being given by

$$dS/dt \approx \alpha_S F - \beta_S S, \tag{3}$$

where S is the singlet excitons concentration. The singlet exciton steady-state concentration S_{ss}, which is established $\sim 10^{-8}$ sec after the onset of illumination is given by

$$S_{ss} \simeq \alpha_S F \beta_S^{-1} \tag{4}$$

In these equations it is assumed that singlet–triplet interactions are kinetically unimportant. The carrier photogeneration rate G can then be expressed as

$$G = K_{ST} S_{ss} T_{ss} + F\sigma_p T_{ss} = (K_{ST}\alpha_S\beta_S^{-1} + \sigma_P)(f\alpha_S/\gamma_T)^{1/2} F^{3/2}, \tag{5}$$

where K_{ST} is the rate constant for bimolecular singlet–triplet interactions that result in the dissociation of a pair of charge-carriers and σ_p is the cross-section for triplet exciton photoionization. For sufficiently high voltages such that every carrier photogenerated near one of the electrodes is collected at the counter electrode (see Figure 4 below) the photocurrent density J is given by

$$J = -q(1/\alpha_S)G = -q\{K_{ST}\beta_S^{-1}(f\alpha_S/\gamma_T)^{1/2} + \sigma_P(f/\alpha_S\gamma_T)^{1/2}\}F^{3/2}. \tag{6}$$

One should note that not only α_S but also f,[15] and σ_p,[3] could be wavelength dependent. Moreover, the second term in Eq. (6), which corresponds to photoionization of triplet excitons, would show a dip in the spectrum where $\alpha_S(\lambda)$ has a peak (if σ_p and f remain constant). Therefore, though the initial step of carrier generation could be the excitation of a singlet exciton, the photocurrent spectrum could still fail to reflect the singlet absorption structure. From our measurements one cannot decide which of the processes, singlet–triplet exciton interaction or triplet photoionization is dominant, however one can estimate upper limits for both K_{ST} and σ_p. From the experimental results of Figures 1–3 we find $K_{ST} \leq 10^{-11}$ cm^{3}sec^{-1} and $\sigma_p \leq 10^{-14}$ cm^2.

We can also consider what would be the result of the same photogeneration processes on the photocurrent following excitation by very short light pulses, such as used in the pulsed photoconductivity study.[6] It can be shown that during these short light pulses, even under the strong light intensities used, (5×10^{23} photons/cm^2 sec, see Ref. 6) neither triplet–triplet, triplet–singlet interactions, nor triplet photoionizations appreciably affect the triplet or singlet exciton concentrations. The average triplet and singlet exciton concentrations are given by $T_{av} \approx f\alpha_S F\tau$ and $S_{av} \approx \alpha_S F\beta_S^{-1}$, respectively. The initial photocurrent density $J(t = 0)$ as measured about ~ 0.2 μ sec following the light pulse (0.2 μ sec was the resolution time of the circuitry) would be given by

$$J(t = 0) = -q(1/\alpha_S)G\tau t_T^{-1} \approx -qf\tau(\sigma_P + k_{ST}\alpha_S\beta_S^{-1})\tau t_t^{-1}F^2. \tag{7}$$

Indeed, a square light intensity dependence such as predicted by Eq. (7)

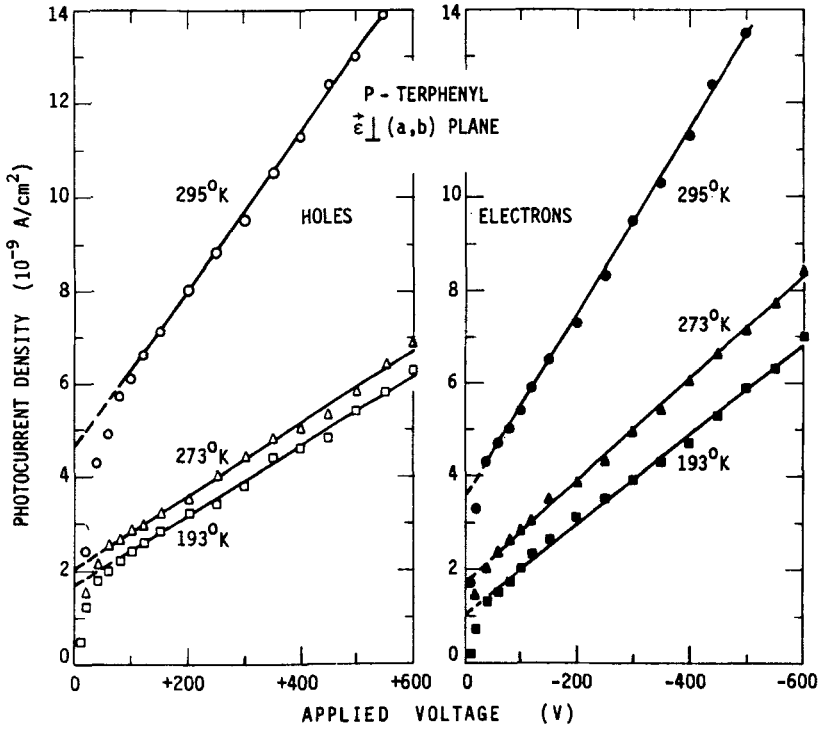

FIGURE 4 Hole and electron photocurrent density vs. voltage plots for various temperatures taken with unpolarized light at $\lambda = 332$ Å ($h\nu = 3.73$ eV) of intensity $F = 9.3 \times 10^{12}$ photons cm^{-2} sec^{-1}. Electric field normal to (a, b) plane; sample thickness 0.15 mm. Voltage polarity refers to illuminated front electrode.

was observed.[6] But, the values of σ_p or K_{ST} which explained the photocurrents under continuous illumination would here predict initial photocurrent densities of the order of 10^2A/cm^2 for light intensities of $\sim 5 \times 10^{23}$ photons/cm^2 sec, while the maximum measured were of the order of 10^{-3}A/cm^2. This difference is probably because the time duration of the excitation pulse, 10^{-8} sec, is sufficiently short that equilibrium conditions do not apply, which is obviously true for triplet exciton populations and distributions. Such effects could become important if, for example, singlet → triplet intersystem crossing in this surface region occurred mainly from trap sites. Naturally the density and distribution of these sites would be less important in steady state experiments for example if triplet detrapping times from such sites was long compared to 10^{-8} sec. Similarly if one of the participating excitons has to be trapped in the surface region, then the number and surface density of such sites would be a limiting condition. Some evidence for the importance of the latter is seen in the effect of light polarization [different

absorption coefficients hence exciton density distribution] on the magnitude of the steady state photocurrents J_a and J_b. A *p*-terphenyl crystal is monoclinic with 2 molecules per unit cell, space group $p^2_{1/a}$.[9] The light absorption polarization ratio for such a crystal symmetry is given by

$$\alpha_a/\alpha_b = \{\mathbf{M}_1 + \mathbf{M}_2) \cdot \mathbf{U}_a/[\mathbf{M}_1 - \mathbf{M}_2]\}^2$$

where $\mathbf{M}_1$ and $\mathbf{M}_2$ are the optical transition moments of the first and second molecules in the unit cell respectively, and $\mathbf{U}_a$ is a unit vector along the **a** crystal axis.[16] To a first approximation $\mathbf{M}_1$ and $\mathbf{M}_2$ can be taken to be identical to isolated molecules transition moments. In *p*-terphenyl a molecular transition moment directed along the long molecular axis, will then result in an infinite polarization ratio, and a molecular transition moment along the short axis, in a polarization ratio 1 : 2.2. The steady state photocurrents J_a and J_b should reflect this polarization ratio, however the carrier generation process power dependence on incident photon density shows a direct comparison is tenuous, to say the least. It seems more probable that the difference in effective surface state densities for the absorption $\|\mathbf{a}$ and $\|\mathbf{b}$ are also of great importance.

We consider next the effect of the electric field on the carrier photogeneration rate. Figure 4 shows some photocurrent density vs. voltage curves for holes and electrons in the temperature range 190–300°K. Initially, all photocurrents rise fast with increasing voltage but then, above 50–70 V, the rise becomes much slower. In the pulsed photoconductivity studies,[6] using samples cut from the same ingot, both hole and electron trapping times were found to be about 1μ sec. Under continuous illumination conditions, all these traps are likely to be filled, hence ineffective for further trapping. Therefore, every carrier ejected into the bulk at one end of the crystal can reach the other end without being trapped. (Our measuring method eliminated the slow trapping, as mentioned in the beginning of this section.) We therefore interpret the inflection voltage $V_{sat} \simeq 50$–70 V as the saturating voltage necessary for the carriers to escape surface recombination, namely[17] $s \simeq \mu(V_{sat}/L)$, where s is the surface recombination velocity, μ is the carrier mobility and L is the sample thickness. Setting[6] $\mu_n = 0.3$ $\text{cm}^2/V \cdot \text{sec}$ and $\mu_p = 0.8$ $\text{cm}^2/V \cdot \text{sec}$, where μ_n and μ_p are the room temperature electron and hole mobilities, respectively, normal to the (a, b) plane, then the surface recombination velocities of electrons and holes, respectively, are $\sim 10^3$ cm/sec and $\sim 3 \times 10^3$ cm/sec. The photocurrents at voltages higher than ~ 100–200 V must reflect the increase in carrier photogeneration rate. This effect relates to the fact that a pair of charge carriers which have been produced with sufficient energy to dissociate, could still recombine due to their mutual coulomb attraction ("geminate recombination").[4] Onsager[5] calculated the dissociation probability of a pair of charge

carriers thermalized at a distance **r** under the action of an external field *E*. For an isotropic medium, and under reasonable assumptions for the distribution of *r* values, the charge separation current can be expressed as[4]

$$J = J_0 \exp(-E_a/k_B T)[1 + AE],$$
$$E_a = (1/4\pi\varepsilon_0)(q^2/\varepsilon_r^{r_0}); \qquad A = (1/4\pi\varepsilon_0)(q^3/2\varepsilon_r(k_B T)^2), \tag{8}$$

where ε_r is the relative dielectric constant of the medium, k_B is Boltzman's constant and r_0 is the average thermalization distance. The basic features predicted by Eq. (8) are: (i) The generation rate should change linearly with voltage with a non-zero intercept at zero voltage. (ii) The zero-field intercept should be thermally activated. A fair agreement with theory has been obtained for pulsed photoconductivity in both anthracene[4] and *p*-terphenyl.[6]

It is seen, in Figure 4 that indeed the basic predictions of Eq. (8) are fulfilled. The zero-field photocurrent density is obtained from extrapolation of the high voltage J–V curve, and this value increases with increasing temperature. To further analyze the temperature dependence of the charge carrier generation, in Figure 5 are shown the zero field photocurrent density, and the product T^2AL^{-1} as functions of $1000/T$, on a semi-log scale. Equation (8) suggests that the former should follow a straight line with a slope $(-Ea)$, while the latter should be independent of temperature. These features are fulfilled only approximately. The values of T^2A/L are indeed independent of temperature, within the experimental error. On the other hand, the results for electrons are consistently higher than those for holes. Separate values for ε_r are thus obtained from the hole and electron photocurrents, 2.1 and 1.4, respectively. A similar analysis of the voltage and temperature effect on carrier generation in pulsed photoconductivity[6] also gave higher values of T^2A/L for electrons. As to the thermal activation, the assignment of an activation energy to the data is not clear. It seems that the zero field photocurrent intercept vs $1000/T$ curve (upper part of Figure 5) flattens at low temperatures. At higher temperatures an activation energy of 0.13 eV can be derived, similar to that obtained in the pulsed photoconductivity studies[6] (0.1 eV). The thermalization distance r_0 is then estimated as 40–70 Å for holes and electrons, if the corresponding values of ε_r are taken from the figure (Figure 5). If the thermalization distance r_0 depends on temperature it would cause a deviation of the plot from a simple thermally activated process. This could be the reason for the flattening of the curve at lower temperatures if r_0 increased with decreasing temperature. It should be noted that if the absorption coefficient α_S or any other parameter characterizing the carrier generation that appears in Eq. (6) changes with temperature, it could also affect the temperature dependence of the photocurrent zero-voltage intercept, but not its voltage dependence. Perhaps this is the reason

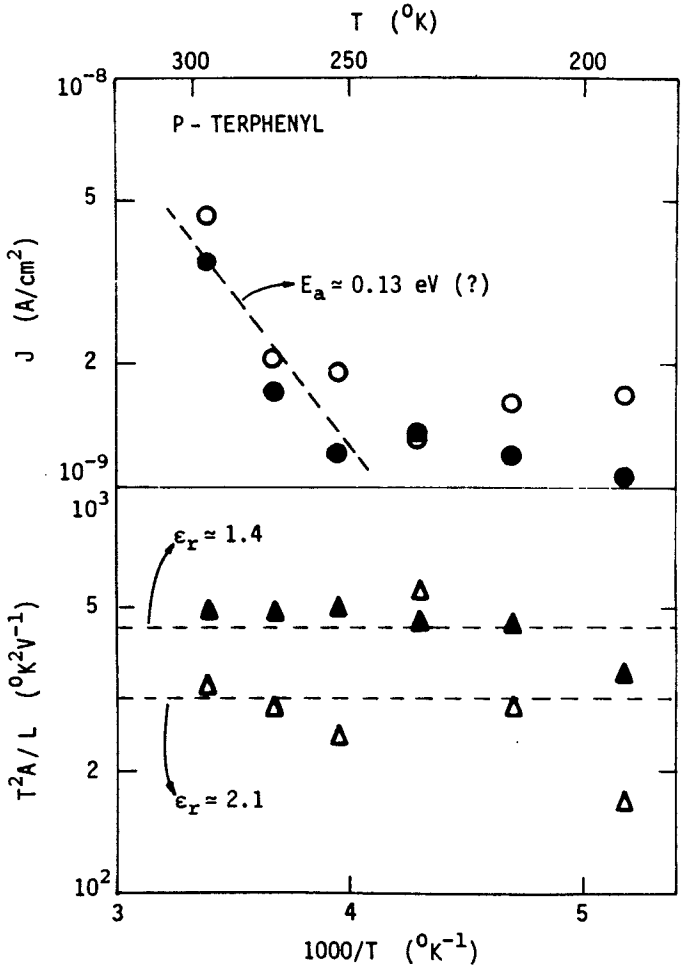

FIGURE 5 Semi-log plot of zero-field photocurrent density (top) and T^2A/L (bottom) vs $1000/T$ for holes and electrons (open and full symbols, respectively). Includes data taken from Figure 4.

why the predicted temperature dependence of T^2A/L is approximately fulfilled over the entire temperature range (with the exception of the discrepancy between the results for holes and electrons), while that of the zero field intercept is not (Figure 5). We hope that the present work will stimulate more work concerning the spectral shape of the absorption coefficient α_S and its temperature dependence as well as the other parameters which might affect charge carrier generation in *p*-terphenyl (Eq. (6)).

IV SUMMARY

This work presents a study of d.c. photoconductivity of *p*-terphenyl single crystals. It was seen that electrons and holes are produced at equal rates both being proportional to the 3/2 power of the light intensity. The spectra show a fast exponential rise of the generation rate (40–50 times) in the photon energy range 3.5–3.73 eV, which is then followed by a plateau up to a photon energy of 4.25 eV. The **b** polarized light is 6–9 times more efficient in carrier production compared to **a** polarized light. These features are discussed in terms of two possible charge-carrier generation mechanisms: (i) bimolecular interaction of photogenerated singlet excitons with triplet excitons, the latters having been produced from the formers by intersystem crossing (ii) by photoionization of triplet excitons produced the same way. Upper limits of 10^{-11} cm^3 sec^{-1} and 10^{-14} cm^2 were estimated for K_{ST} and σ_p, the singlet triplet interaction rate constant and the triplet photoionization cross section, respectively. The photo-current density vs voltage curve is shown to be controlled by surface recombination at low voltages, with surface recombination velocities of $\sim 3 \times 10^3$ cm/sec and $\sim 10^3$ cm/sec for holes and electrons, respectively. For higher voltages, the electric field affects the carrier generation rate itself, and this has been studied as function of temperature. The general features are shown to be in agreement with the basic predictions of Onsager's theory. The photocurrent increases linearly with voltage, with a non-zero intercept at zero voltage, which is thermally activated. Slight departures from the theory are attributed to the effect of temperature on the singlet absorption coefficient or any of the other parameters and cross-sections which determine the carrier generation rate.

References

1. J. Gonzalez-Basurto, Z. Burshtein, and J. Levinson, *Mol. Cryst. Liquid Cryst.*, **31**, 131 (1975).
2. J. W. Steketee and J. de Jonge, *Philips Res. Repts.*, **17**, 363 (1962).
3. A. Bergman and J. Jortner, *Phys. Rev.*, **B9**, 4560 (1974).
4. R. R. Chance and C. L. Braun, *J. Chem. Phys.*, **64**, 3573 (1976).
5. L. Onsager, *Phys. Rev.*, **54**, 554 (1938).
6. Z. Burshtein and D. F. Williams, *J. Chem. Phys.*, **68**, 983 (1978).
7. O. H. LeBlanc, Jr. in *Physics and Chemistry of the Organic Solid State* (Eds. D. Fox, M. M. Labes, and A. Weissberger), (Interscience, 1967) Vol. III, p. 133.
8. R. C. Sangster and J. W. Irvine, *J. Chem. Phys.*, **24**, 670 (1956).
9. H. M. Rietveld, E. N. Maslen, and C. J. Clews, *Acta Crystallog.*, **B26**, 693 (1970).
10. J. L. Baudour, H. Carleau, Y. Ddugeard, J. Desuche, A. Girard, and J. Meinel, *Mol. Cryst. Liq. Cryst.*, **32**, 5 (1976).
11. J. Kommandeur, G. J. Korinek, and W. G. Schneider, *Can. J. Chem.*, **36**, 607 (1958).

12. J. Birks and A. Cameron, *Proc. Roy. Soc.*, **249**, 207 (1959).
13. M. W. Windsor in Ref. 7, Vol. II, p. 343.
14. P. Avakian and R. E. Merrifield, *Molecular Crystals*, **5**, 37 (1968).
15. M. Chabr and D. F. Williams—to be published.
16. D. P. Craig and S. H. Walmsley in Ref. 7, Vol. I, p. 585.
17. J. Levinson, Z. Burshtein, and A. Many, *Mol. Cryst. Liq. Cryst.*, **26**, 329 (1974).